A TECTONIC MODEL FOR THE NORTHERN LLANOS AND SOUTHERN BARINAS-APURE BASINS

BY

JAMES C. HOWARD

TRUDI WEBB

TOM CHRISTENSEN

SUN EXPLORATION AND PRODUCTION COMPANY

OBSERVATIONS

An examination of drainage patterns in the Llanos Basin of Colombia reveals abrupt changes in direction and character of stream segments, suggesting underlying structural control. Drainage patterns are evident on the geologic map of Colombia, topographic maps of the area and on Landsat imagery (Figure 1).

An examination of Landsat imagery reveals linear features or lineaments in the form of tonal anomalies and stream segments. It is assumed that these lineaments represent tectonic elements detected at the earth's surface.

OBJECTIVE

From these observations, it was decided to determine if there is a correlation between the strike of tectonic elements detected at the surface and in the subsurface, that would reveal the nature of tectonic stresses producing deformation of the sedimentary cover at a regional scale.

DATA BASE

Data used in the study to achieve this objective consist of five Landsat images covering the northern Llanos Basin of Colombia and the southern Barinas-Apure Basins of Venezuela, together with selected seismic coverage in the portion of the Llanos Basin covered by the imagery (Figure 2).

A tectonic "quilt" map was patched together from various seismic interpretations made at different horizons between the Mirador and Cretaceous unconformity levels. The composite map is based on interpretations from several vintages of seismic data, varying in data quality due to differences in acquisition and processing parameters.

Separately, seismic basement representing the shield was interpreted and mapped where possible.

INTERPRETATION

Landsat images were interpreted for lineaments (Figure 3) by Trudi Webb, a geology graduate student who did not have a thorough knowledge of the regional geology, thereby minimizing geological bias in the interpretation.

Trudi analyzed the imagery by recognizing patterns of linear anomalies. Linear features were mapped regardless of length. As a novice imagery interpreter, she therefore also minimized interpretation bias.

Fault patterns were extracted from the two, regional structure maps by Tom Christensen, a geology graduate student who then displayed the fault traces as lineaments, without regard to the nature of offset across or along the fault traces. Figure 4 is a fault trace map constructed from seismic interpretations within the sedimentary cover. Likewise, Figure 5 is a fault trace map constructed from a seismic interpretation of basement.

DATA PROCESSING

Lineaments from both Landsat imagery and seismic data were processed by frequency analysis of lineament azimuths. In each case, results were displayed by the computer in the form of histograms and rose diagrams along with a plot of actual lineament lengths and directions (Figure 6).

The rose diagram permits a visual comparison of directions for lineaments. Landsat and seismic data can be compared readily by means of a rose diagram (Figures 7 and 8). Another use of the rose diagram is to compare lineament directions to orientations of deformational features associated with tectonic models.

A strain ellipsoid for wrench faulting (Figure 9) provides a tectonic model that fits the rose diagrams for imagery and seismic derived lineaments. The strain ellipsoid shows relative relationships and orientations for deformational features such as strike-slip faults, normal faults, reverse or thrust faults and folds created by tectonic compression or by a differential, rotational couple.

RESULTS

Both imagery and seismic data reveal a prominent NE trend of lineament strikes. When superimposed, the rose diagrams demonstrate a direct overlay of the most prominent NE lineament directions. (Figure 10).

When superimposed on drainage patterns, the strain ellipsoid for an E-W compression shows a good fit between stream directions, strike-slip directions and tensional fault directions (Figure 11).

There is an excellent correspondence between the most frequent lineament directions for lineaments detectable from imagery and the primary strike-slip directions associated with an E-W compression (Figure 12). The imagery reveals a slightly less prominent NW striking trend of lineaments. The acute angle separating the NE and NW trends is approximately 60 degrees. The line bisecting this angle is oriented almost due E-W.

A strain ellipsoid for wrench faulting, created by an E-W compression fits the rose diagram for imagery derived lineaments (Figures 9 and 12). Directions for synthetic, right lateral and antithetic, left lateral strike-slip faults overlie the prominent NE and NW frequency trends of the rose diagram. Associated with this wrench model, N-S striking folds and E-W striking tensional faults overlie less prominent N-S and E-W trends depicted by the rose diagram for frequency of lineament directions.

An alternate explanation for the frequency of lineament directions seen on imagery is that the wrench model fits the dominant frequency trends, by assuming a recent episode of E-W compression. The strain ellipsoid can be rotated by almost 90 degrees to fit a secondary or less dominant frequency trend in the rose diagram, (Figure 13). This fit implies either an earlier or weaker episode of nearly N-S compression resulting in NNW-SSE oriented, synthetic, right lateral, and NNE-SSW oriented, antithetic, left lateral faults. Associated with this wrench model, E-W striking folds and N-S striking tensional faults overlie the less dominant E-W and N-S trends on the rose diagram respectively.

Seismic data reveal a prominent NE trend of fault strikes in the sedimentary cover but the complimentary NW trend, seen at the surface, is absent (Figure 14). Instead, a less prominent NNE striking trend is obvious within the sedimentary section. This NNE trend can be explained by a second-order, right lateral wrench fault system caused by reorientation of the principal horizontal stress as deformation proceeds along a primary, NW oriented, left lateral wrench fault. However, expression of the NW oriented wrench fault is not apparent in the data.

A plausible explanation for the apparent absence of the NW lineament trend in seismic data and its presence on the imagery is that when deformation occurs it commonly proceeds on only one of the two possible strike-slip directions. However, subtle compaction effects in the NW strike-slip direction could leave it opaque to seismic detection, whereas differential compaction of the sediments could manifest itself as tonal contrasts on the imagery.

Fault patterns in basement also reflect a prominent NE striking trend (Figure 15). In terms of a wrench model, this trend corresponds to a right lateral, synthetic, strike-slip direction due to an E-W compression (Figure 16). Again, no NW direction is apparent.

Rose diagrams for each of the five images reveal significant differences from one image to another in a direction away from the Andes foothills across the sedimentary basins and toward the Guayana shield (Figure 17). The most frequent lineament directions in the two images closest to and and including the foothills have a strong NW orientation, which may represent drainage from the foothills. The most frequent lineament directions in the images farthest from the foothills display a strong NE orientation, which is likely to be an expression of regional, right lateral wrench zones. Those diagrams for images closest to the shield show a fairly uniform distribution of azimuth frequencies other than the dominant NE direction. Such distribution of dispersed orientations would be expected where the sediment cover thins over the shield. In fact, drainage patterns in the area are dendritic to trellis in character, reflecting the relatively uniform nature of the shield's igneous and metamorphic composition.

The contribution of long, regional lineaments to the overall distribution of lineaments becomes apparent by filtering from the total distribution, only those lineaments that measure greater than six inches on a map scale of 1:250,000, that is those that are longer than 40 kilometers (Figure 18). The result demonstrates that regional lineaments are more frequently oriented to the NW near the foothills and to the NE elsewhere geographically in the basins. In general, regional scale lineaments contribute most to the dominant orientations in the total distribution of lineaments.

Evidence for wrench faulting on a regional scale is seen throughout northern Colombia and Venezuela (Figure 19). For example, the right lateral Bocono fault in the Merida Andes of Venezuela is oriented NE and corresponds to the synthetic, strike-slip direction created by an E-W compression. The right lateral Oca fault and the left lateral Santa Marta fault intersect at an angle of 60 degrees and fit a wrench tectonic model created by a NW-SE compression during Miocene to Pliocene time.

CONCLUSIONS

Prominent, regional elements of tectonic deformation are evident at the earth's surface and within the sedimentary cover, as well as in basement rocks, as detected by Landsat imagery and seismic data. These patterns of tectonic deformation fit a wrench tectonic model (Figure 20).

Deformation patterns consist of tectonic lineaments. A prominent and persistent NE oriented trend that extends from basement through the sedimentary cover to the land surface can be attributed to regional zones of right lateral wrench faulting.

A less prominent and less persistent NW oriented trend of lineaments may be attributed to primary, antithetic, left lateral, strike-slip faults. This trend is apparent on imagery but to a much lesser degree on the seismic data. Near the Andes mountains, long NW oriented lineaments may be tectonic in origin or reflections of drainage or both.

Also apparent on the imagery are drainage controls by tectonic elements grounded in igneous basement.

When fitted to the deformation patterns, a strain ellipsoid for a wrench tectonic model reveals two likely superimposed, regional directions of tectonic stress. A weaker, N-S oriented compression may correspond to an older, more obscure, tectonic event possibly of Paleozoic age. Superimposed on the N-S stress regime is an overprint of deformation corresponding to an E-W compressive stress regime of younger age, likely to be associated with the Plio-Pleistocene, Andean orogeny.

REFERENCES

Campbell, C.J., 1965, The Santa Marta wrench fault of Colombia and its regional setting, 4th Carib. Geol. Conf. Trinidad, p.247-261.

Feininger, T., 1970, The Palestina Fault, Colombia, Bull. G.S.A., V.81, p. 1201-1216.

Harding, T.P., 1974, Petroleum traps associated with wrench faults, Bull. A.A.P.G. v.58, p. 1290-1304.

Irving, E.M., 1975, Structural evolution of the northernmost Andes, Colombia, U.S.G.S. Prof. Paper 846, 47 p.

Moody, J.D. and Hill, M., 1956, Wrench fault tectonics, Bull. G.S.A., v.67, p.1207-1246.

Reading, H., 1980, Characteristics and recognition of strike-slip fault systems, Spec. Publ. Int. Assoc. Sediment., v.4, p.7-26.

Rod, E., 1956, Strike-slip faults of northern Venezuela, Bull. A.A.P.G., v.40, p.457-476.

Von Estorff, F.E., 1946, Tectonic framework of northwestern South America, Bull. A.A.P.G., v.30, p.581-590.


SUN RSL P6.P5.Z COLOMBIA MOSAIC
LANDSAT IMAGE MOSAIC
0 10 20 30 40 50
KILOMETERS

FIGURE 1

IMAGE AND SEISMIC COVERAGE OF LLANOS - BARINAS - APURE BASINS

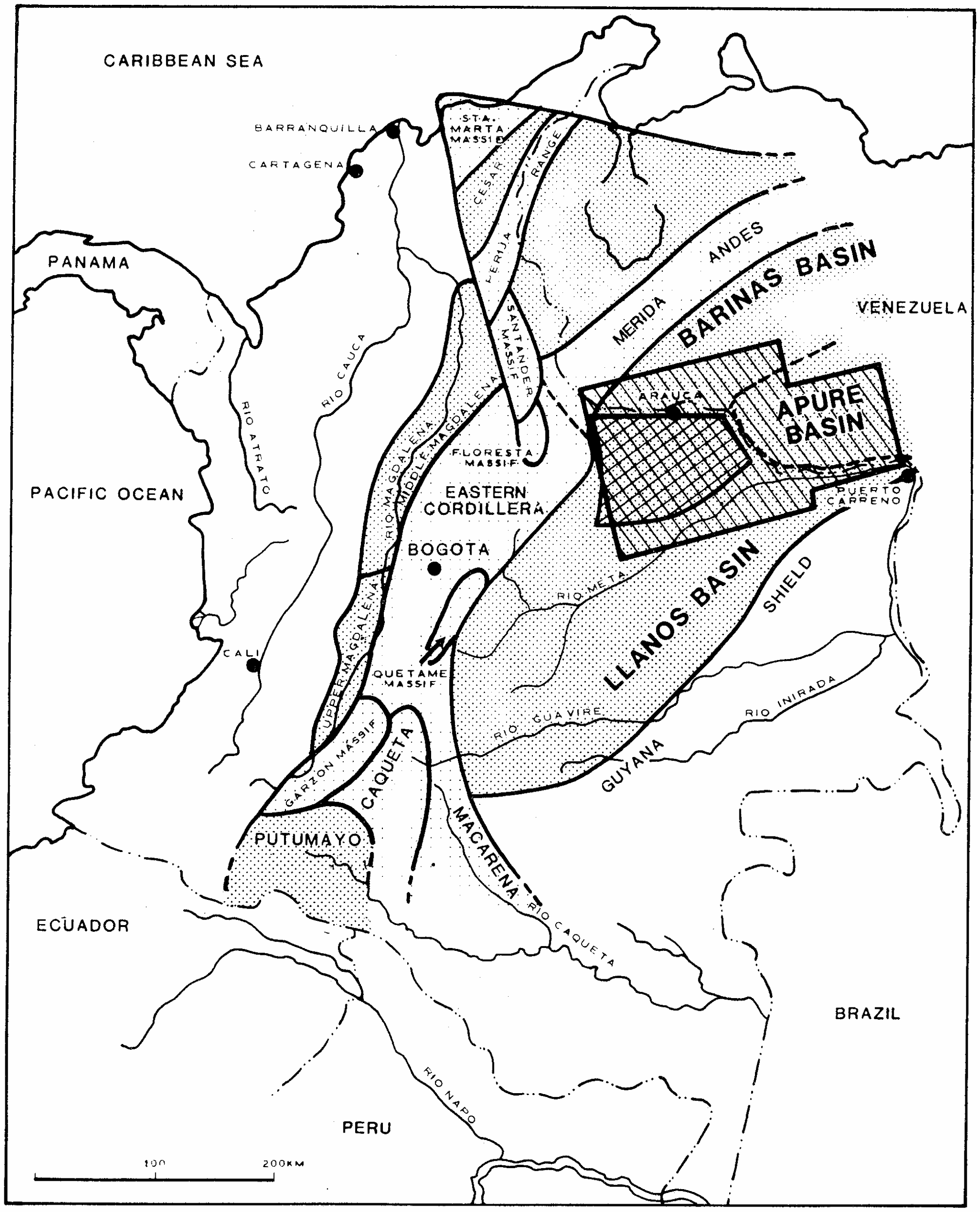

IMAGERY SEISMIC

FIGURE 2

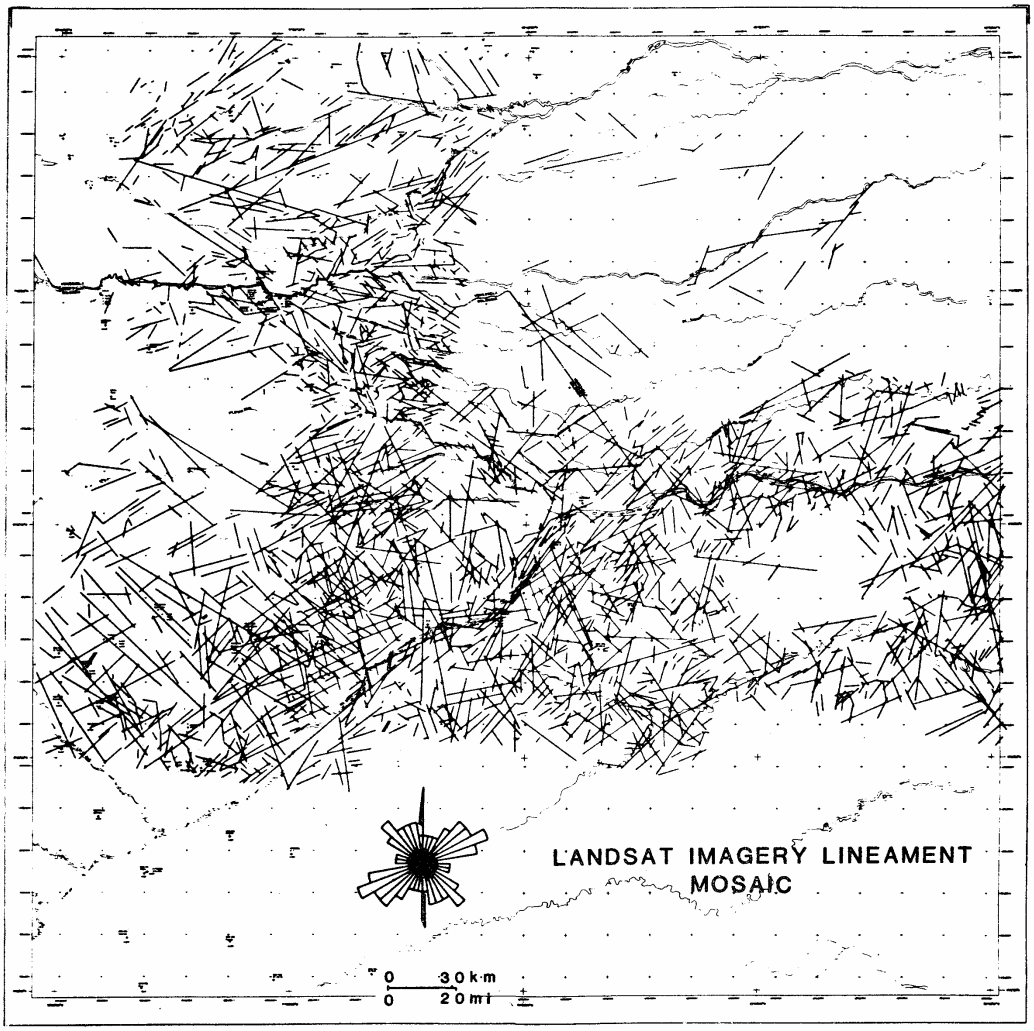

FIGURE 3

SEISMIC FAULT TRACE MAP
MIRADOR-CRETACEOUS INTERVAL

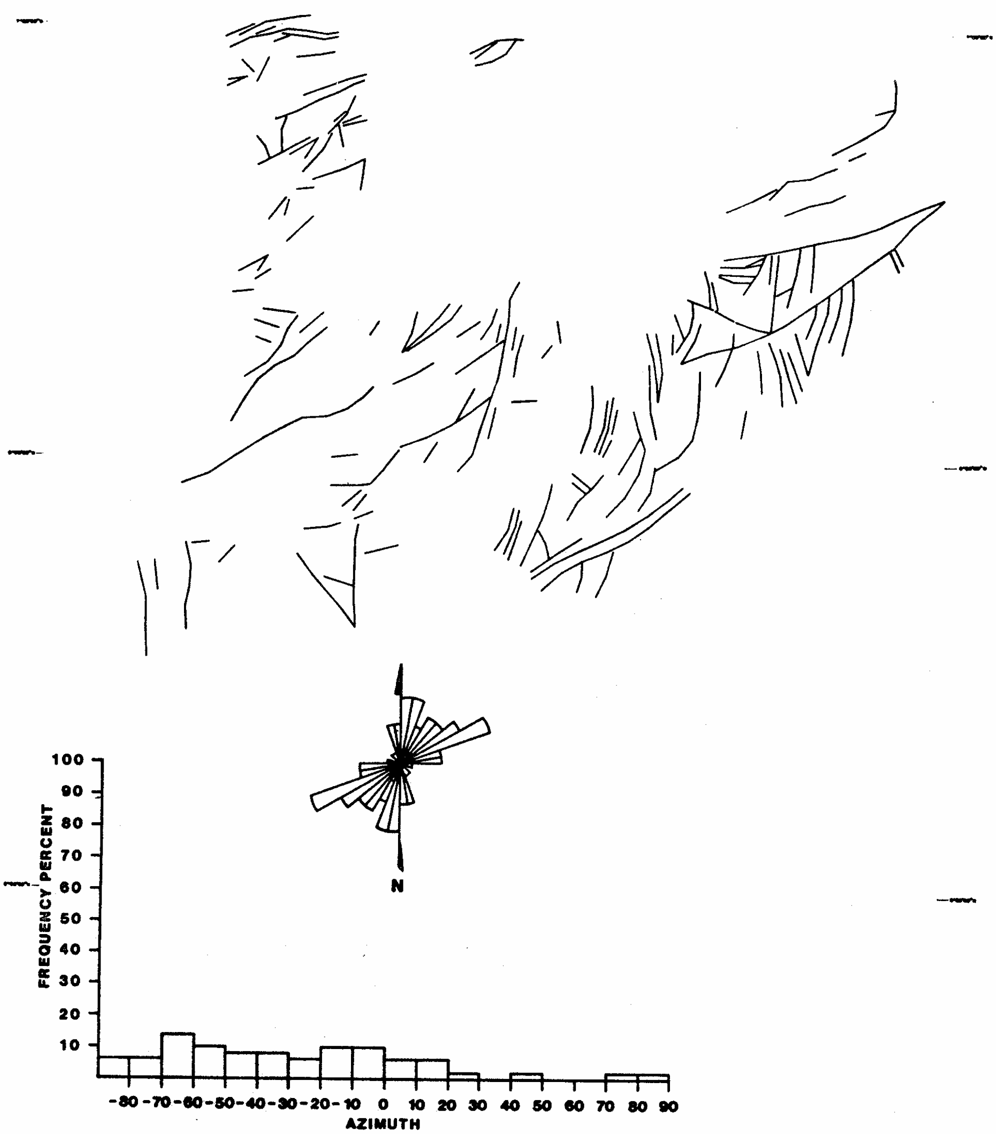

FIGURE 4

SEISMIC FAULT TRACE MAP

BASEMENT

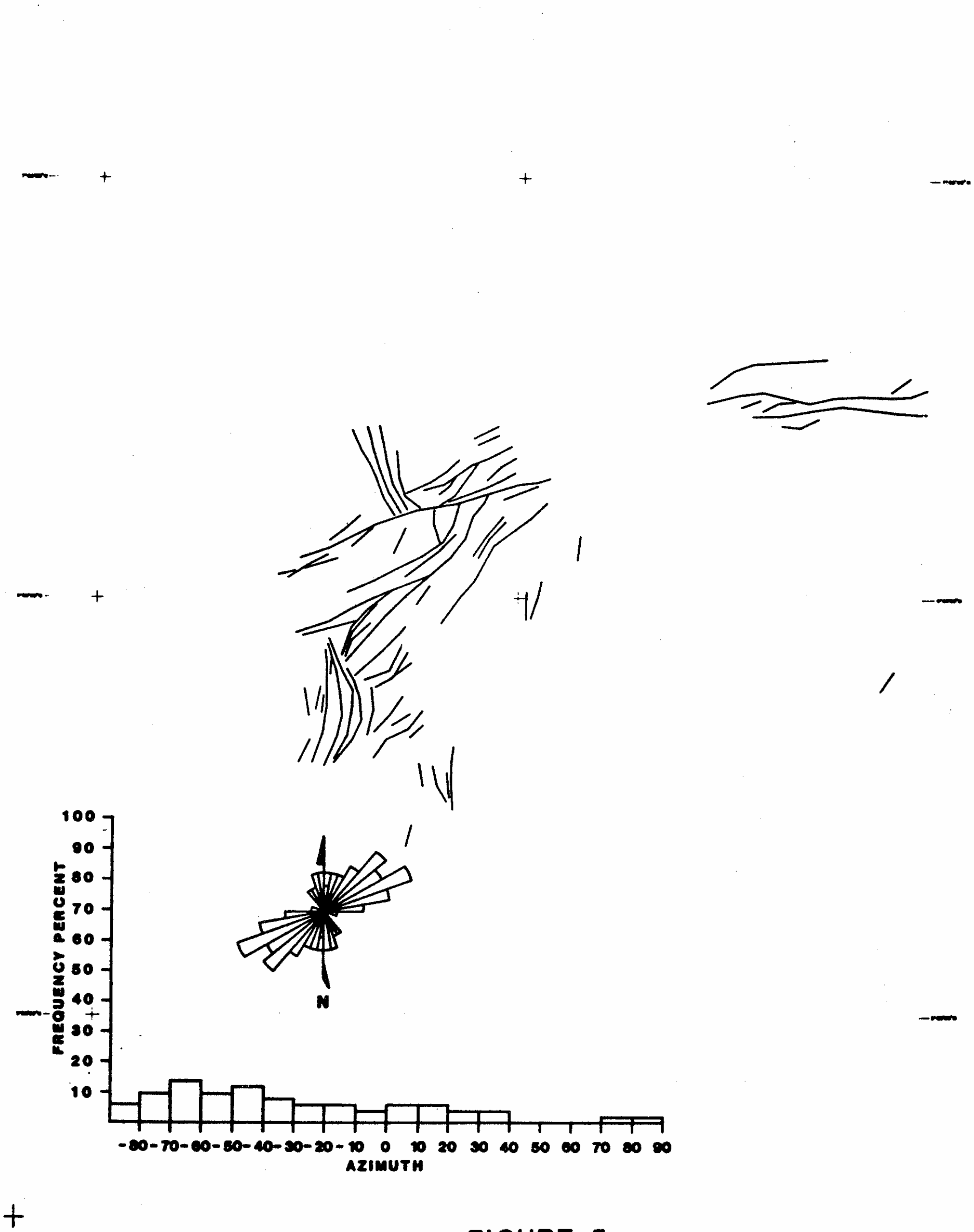

FIGURE 5

LANDSAT IMAGE LINEAMENT P6R56
WITH ROSE DIAGRAM AND HISTOGRAM

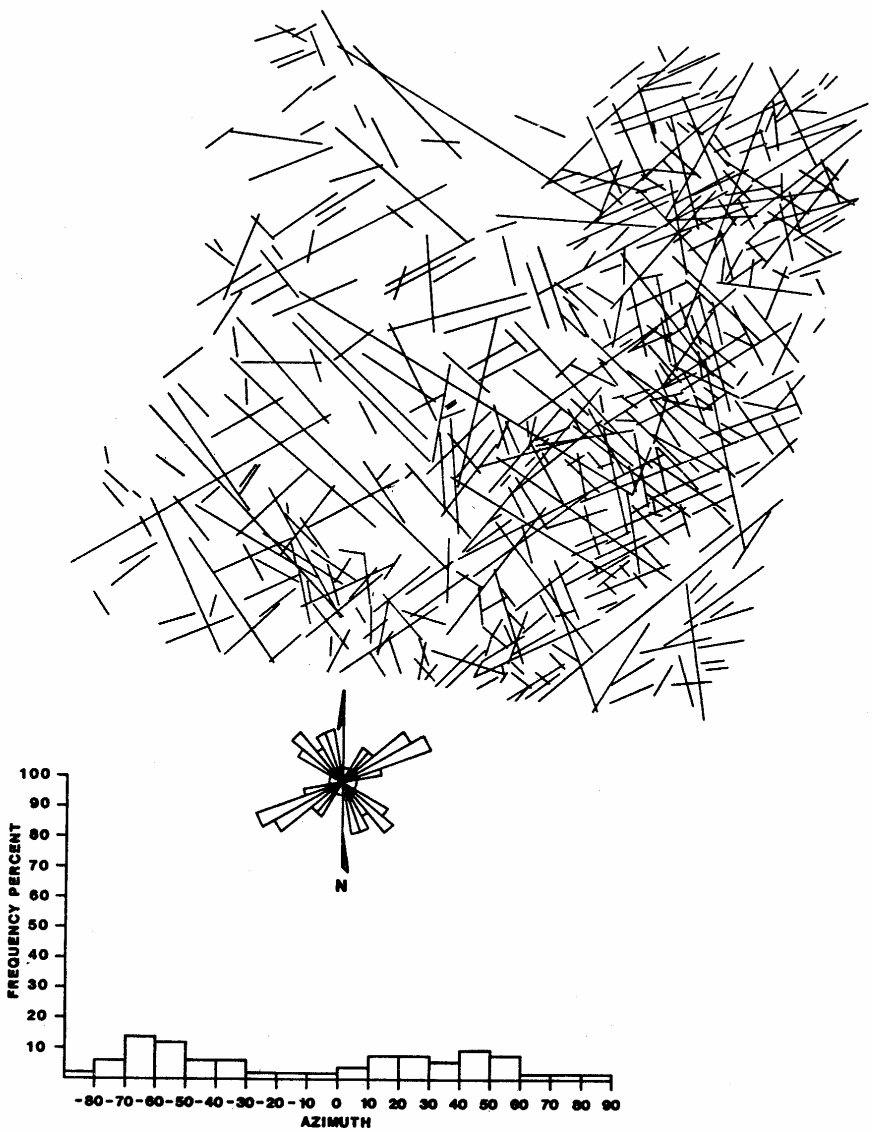

FIGURE 6

LANDSAT

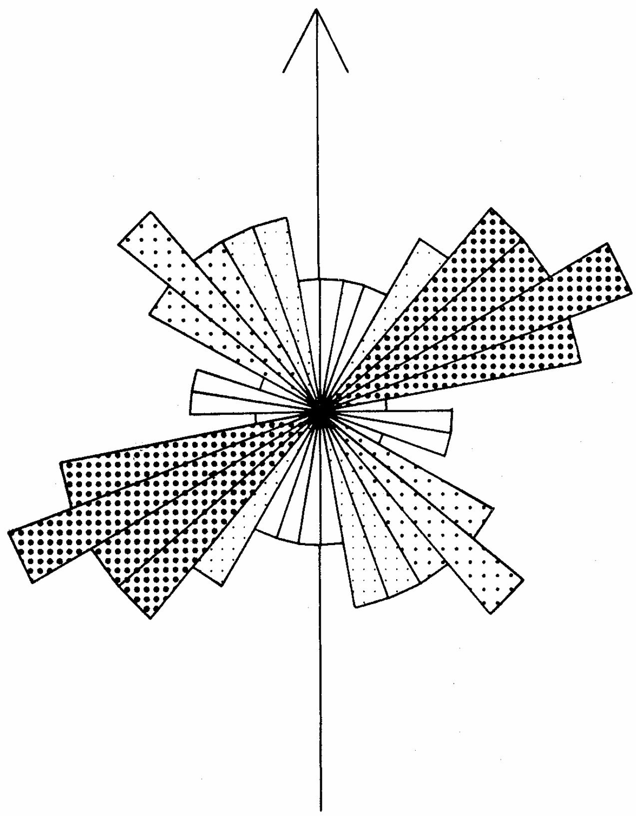

ROSE DIAGRAM
OF
LINEAMENT DIRECTIONS

FIGURE 7

SEISMIC
MIRADOR-CRETACEOUS INTERVAL

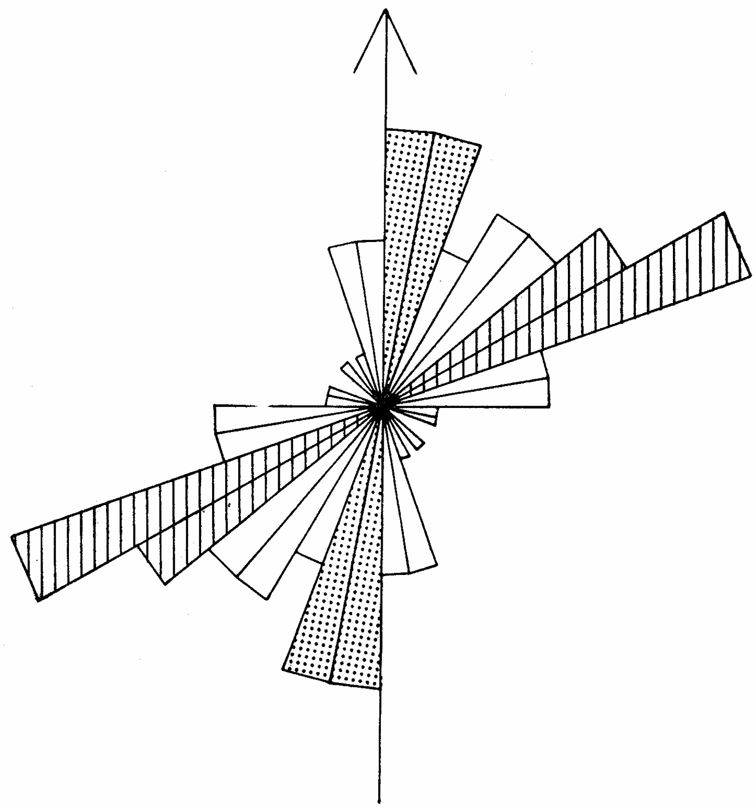

ROSE DIAGRAM
OF
LINEAMENT DIRECTIONS

FIGURE 8

STRAIN ELLIPSOID FOR WRENCH FAULTING

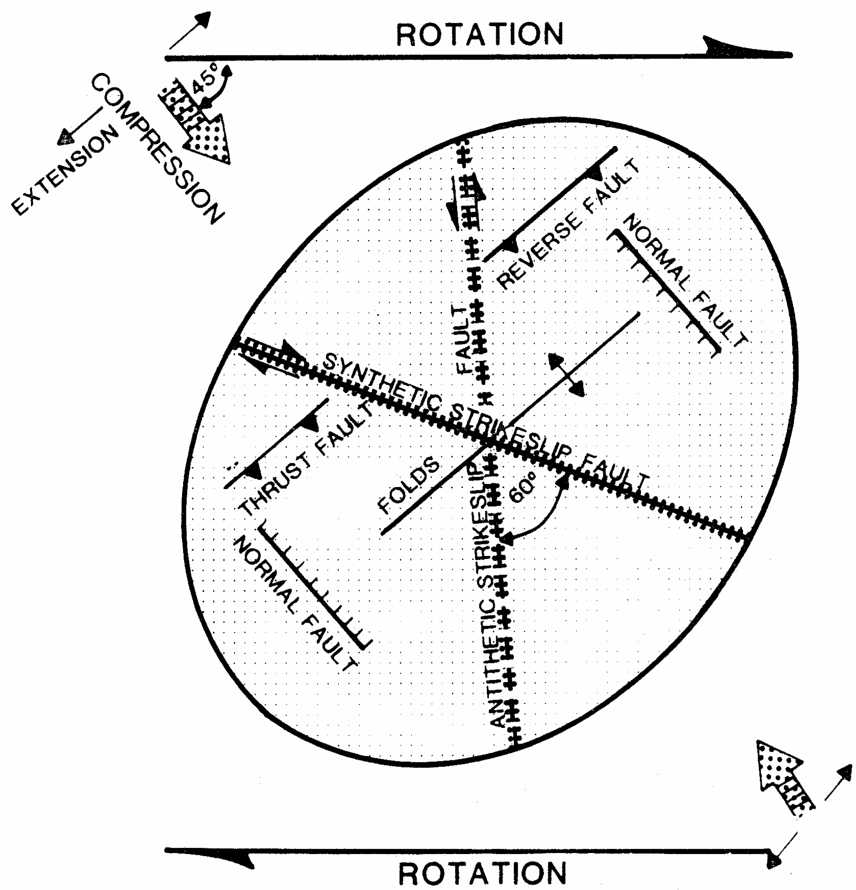

FIGURE 9

OVERLAY OF LANDSAT AND SEISMIC LINEAMENT DIRECTIONS

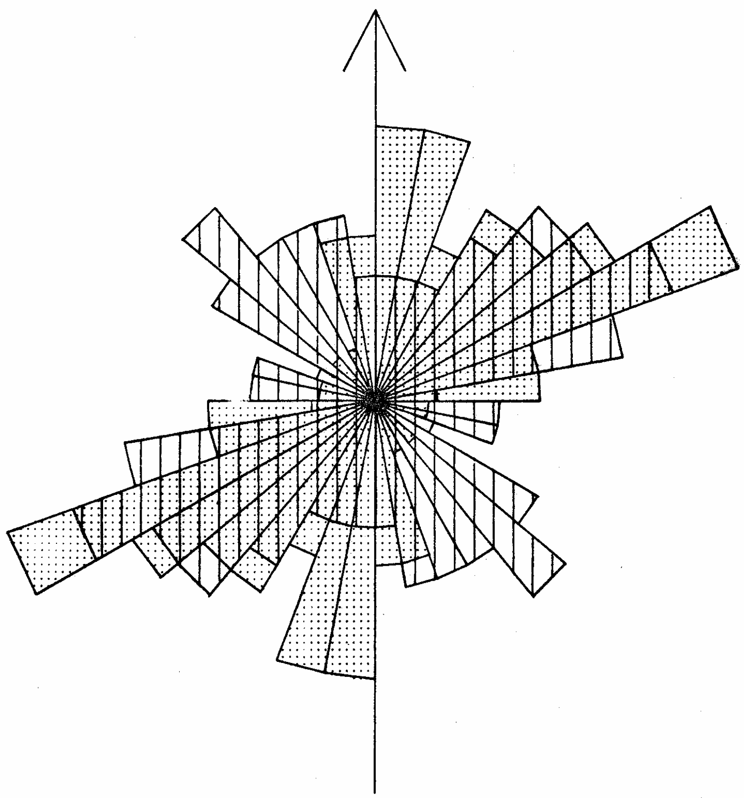

FIGURE 10

WRENCH FAULT STRAIN ELLPSOIDS SUPERPOSED ON DRAINAGE

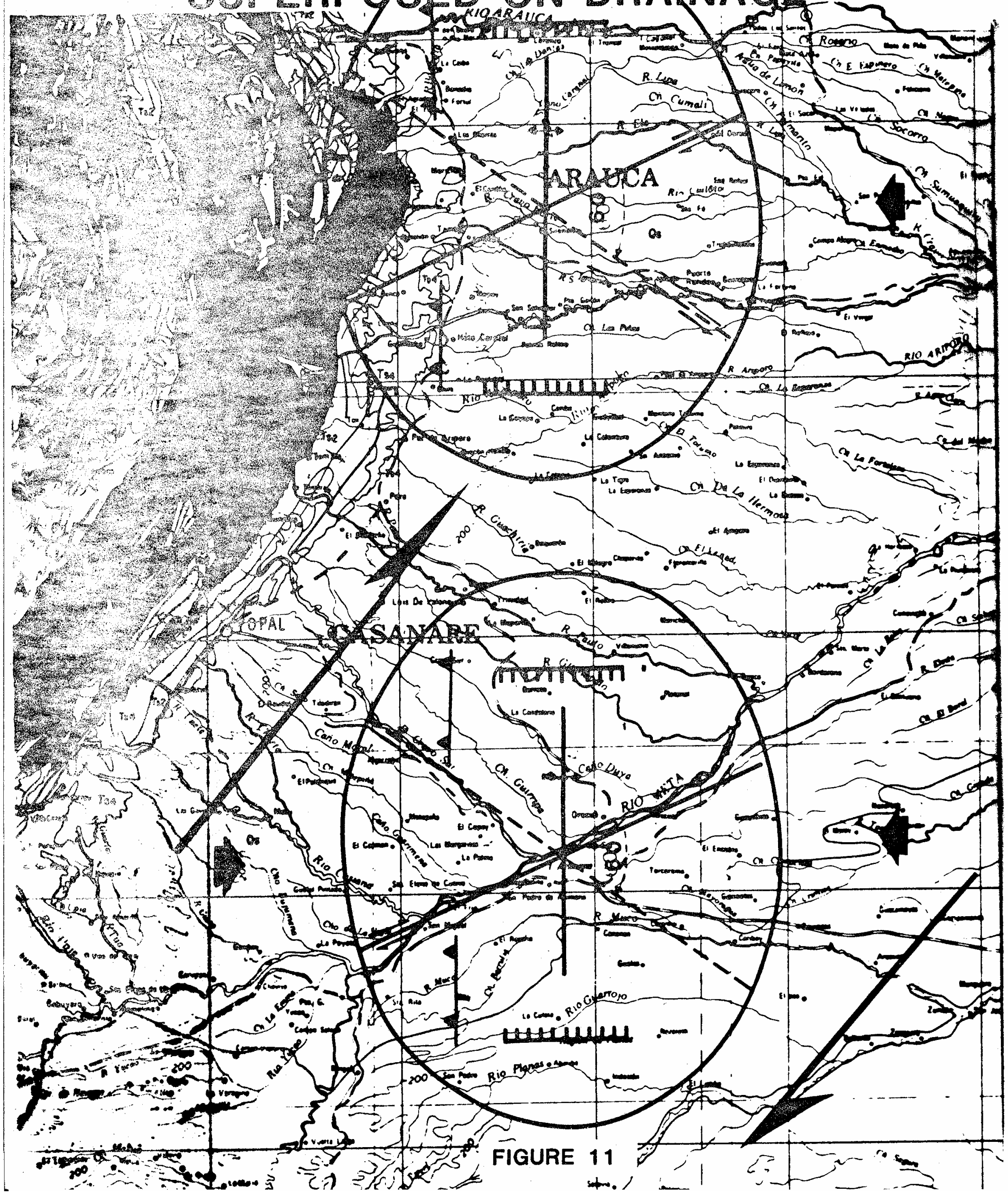

FIGURE 11

LANDSAT

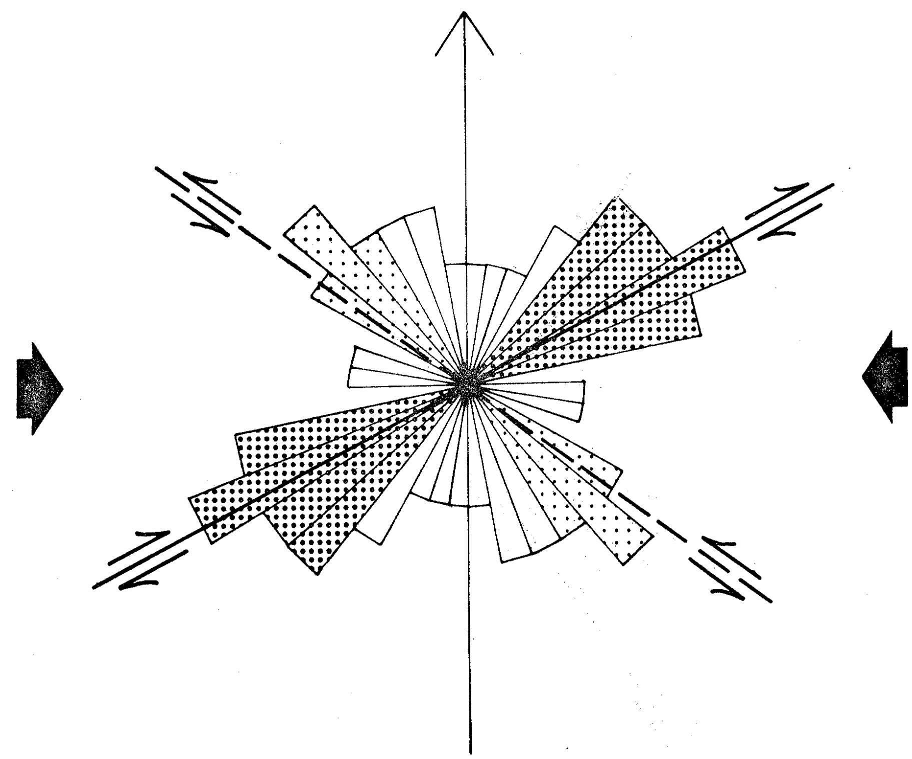

STRIKE SLIP FAULTS CAUSED BY E-W COMPRESSION

FIGURE 12

LANDSAT

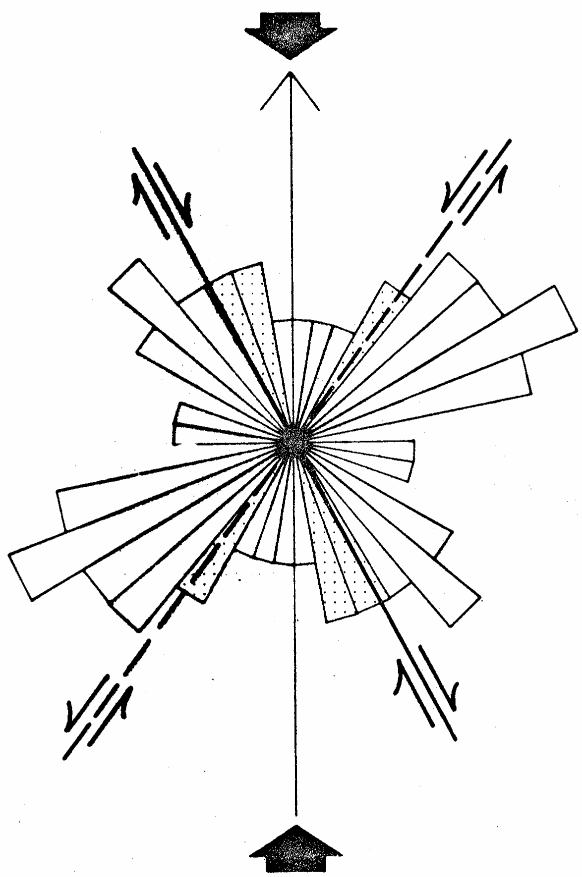

STRIKE SLIP FAULTS CAUSED BY N-S COMPRESSION

FIGURE 13

SEISMIC
MIRADOR-CRETACEOUS INTERVAL

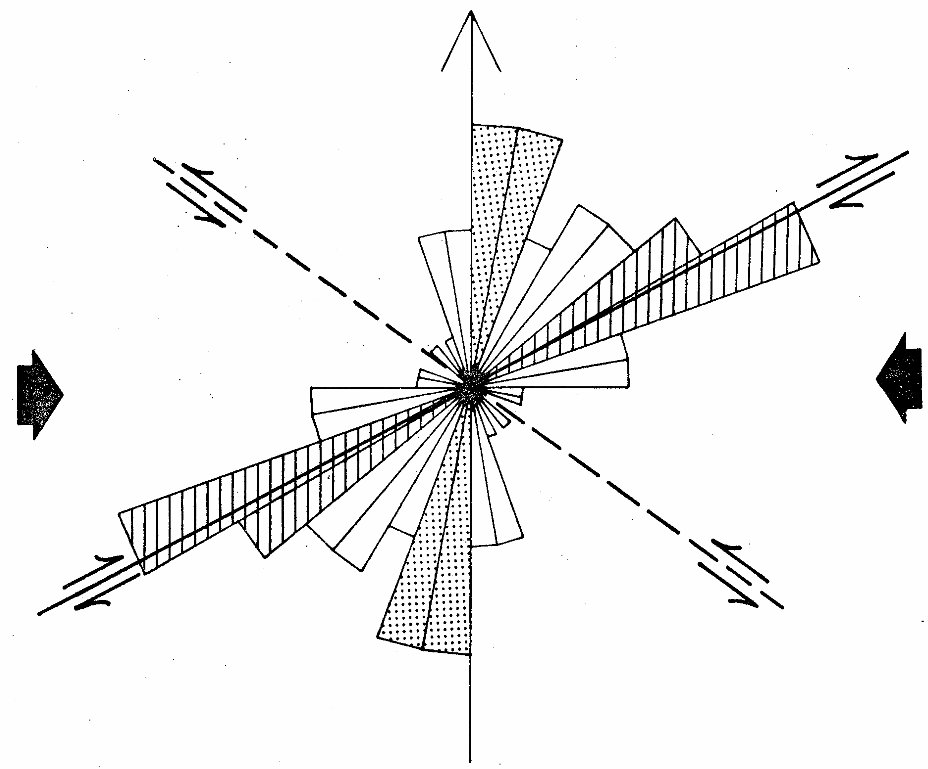

**STRIKE SLIP FAULTS
CAUSED BY
E-W COMPRESSION**

FIGURE 14

SEISMIC
BASEMENT LEVEL

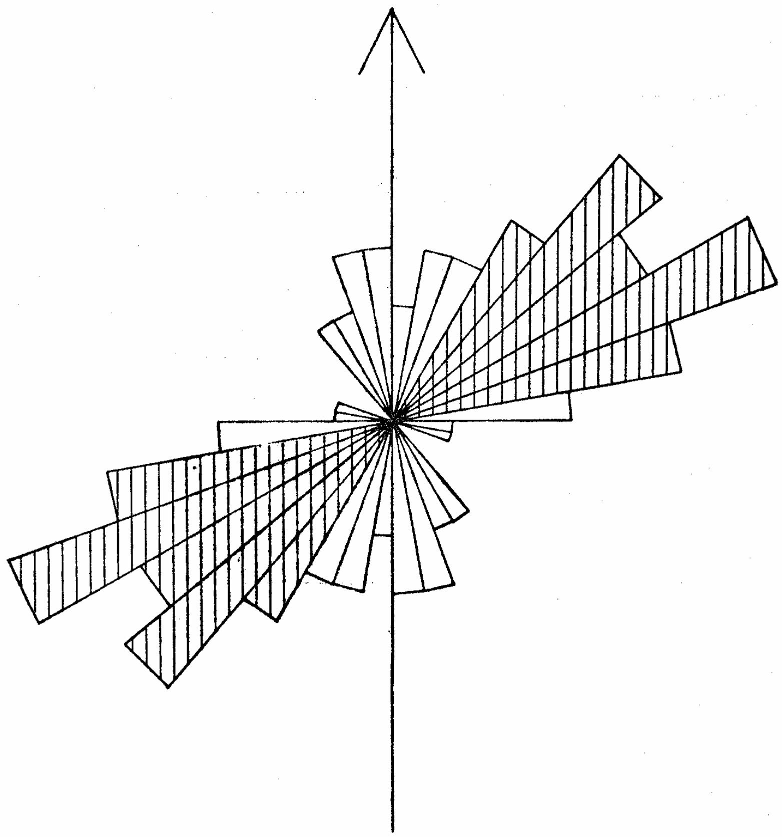

ROSE DIAGRAM OF LINEAMENT DIRECTIONS

FIGURE 15

SEISMIC
BASEMENT LEVEL

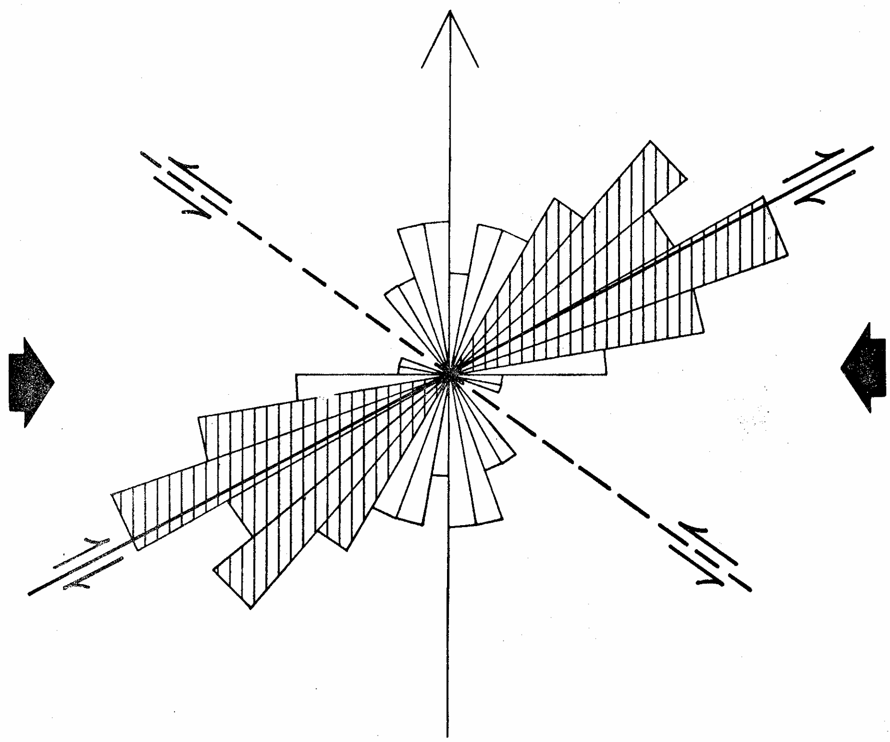

STRIKE SLIP FAULTS
CAUSED BY
E-W COMPRESSION STRIKE

FIGURE 16

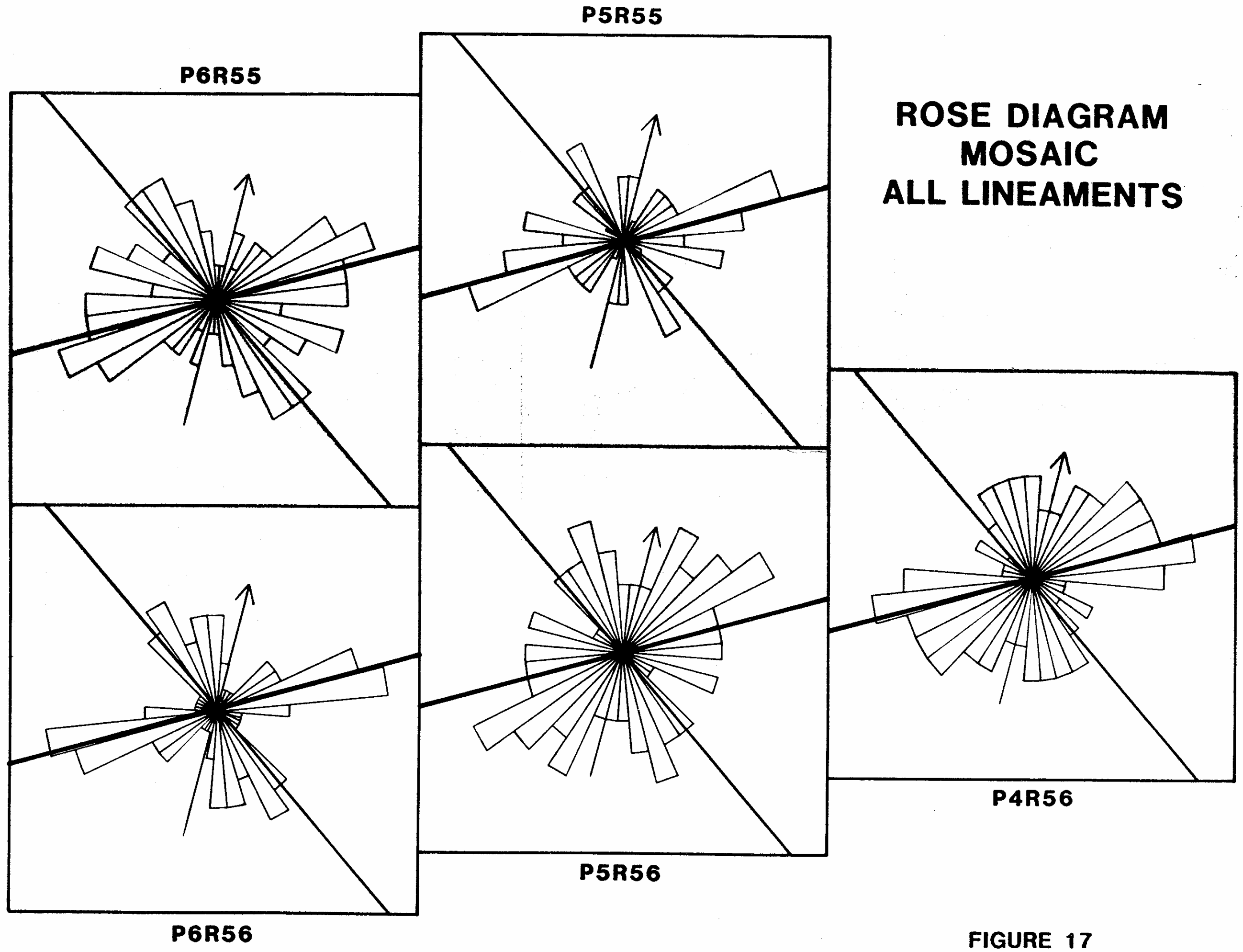

ROSE DIAGRAM MOSAIC ALL LINEAMENTS

FIGURE 17

ROSE DIAGRAM MOSAIC LINEAMENTS GT6

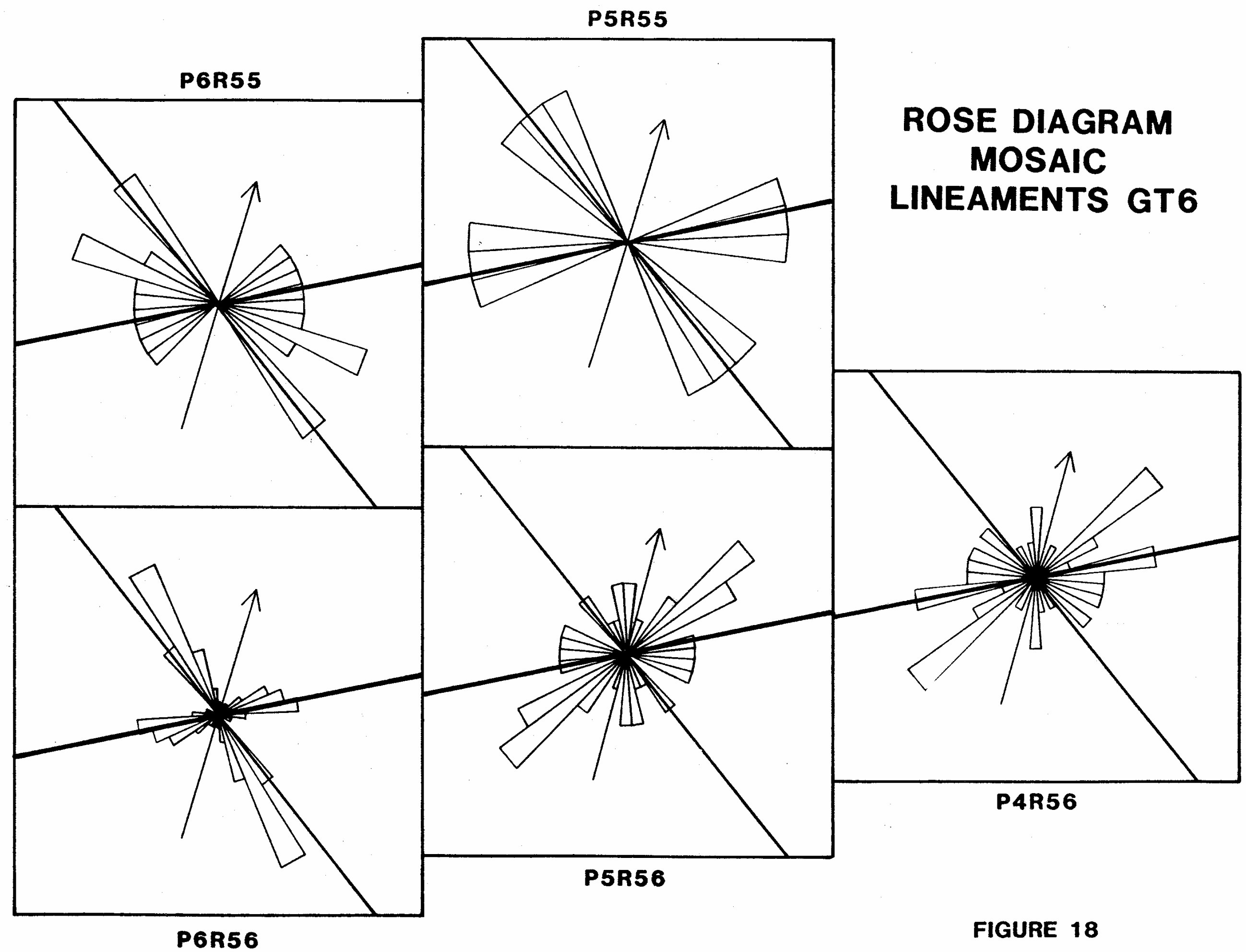

FIGURE 18

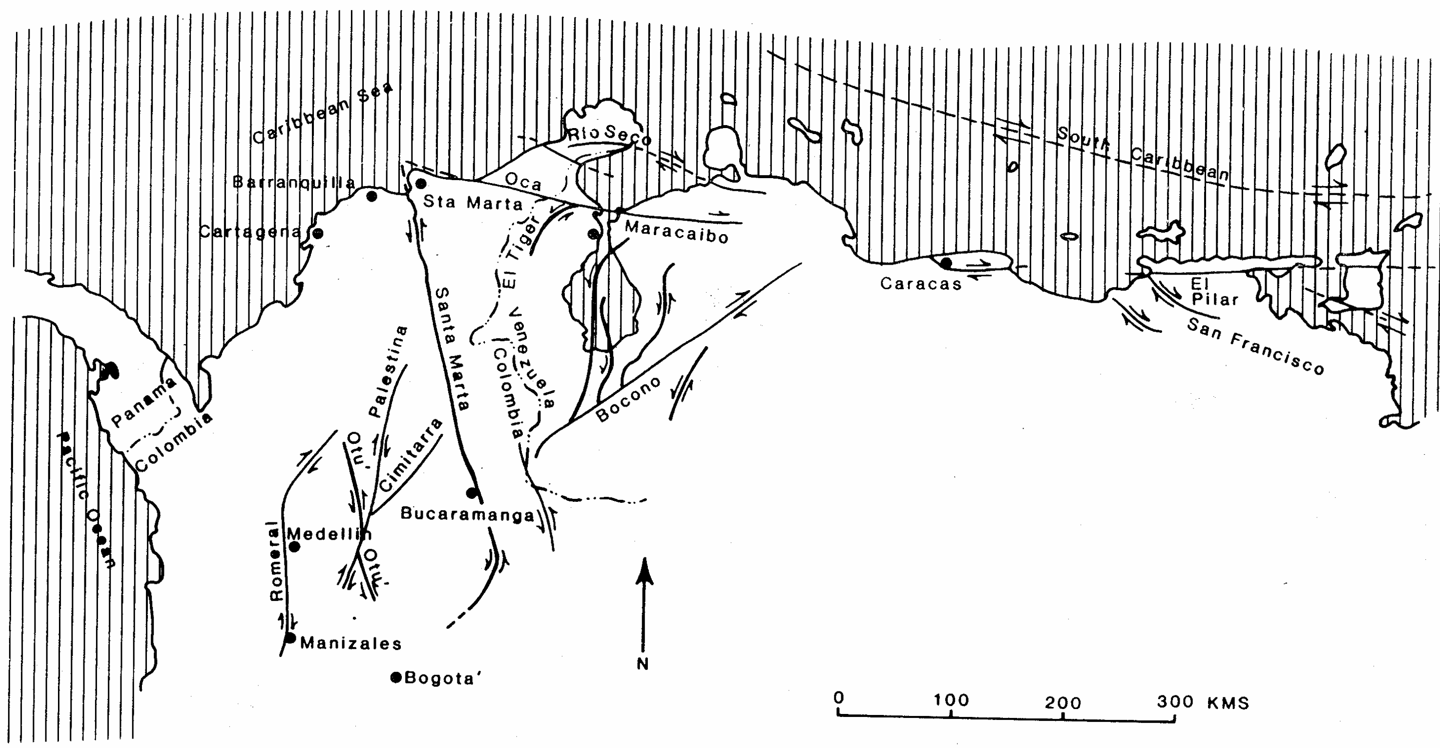

LARGE WRENCH FAULTS NORTHERN COLOMBIA & VENEZUELA

FIGURE 19

WRENCH FAULT TECTONIC MODEL

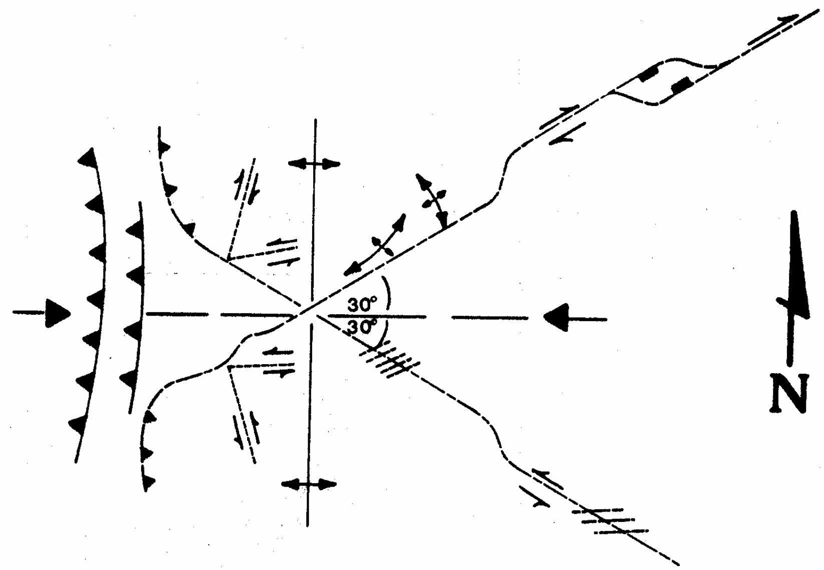

—— PRIMARY FEATURES

- - - FIRST ORDER FEATURES

------ SECOND ORDER FEATURES

FIGURE 20